

## Height fluctuations and intermittency of $V_2O_5$ films by atomic force microscopy

This article has been downloaded from IOPscience. Please scroll down to see the full text article.

2003 J. Phys.: Condens. Matter 15 1889

(<http://iopscience.iop.org/0953-8984/15/12/306>)

View [the table of contents for this issue](#), or go to the [journal homepage](#) for more

Download details:

IP Address: 171.66.16.119

The article was downloaded on 19/05/2010 at 08:29

Please note that [terms and conditions apply](#).

# Height fluctuations and intermittency of $V_2O_5$ films by atomic force microscopy

A Irajizad<sup>1</sup>, G Kavei<sup>2</sup>, M Reza Rahimi Tabar<sup>1,3,4</sup> and S M Vaezi<sup>5</sup>

<sup>1</sup> Department of Physics, Sharif University of Technology, PO Box 11365-9161, Tehran, Iran

<sup>2</sup> Material and Energy, Research Centre, PO Box 14155-4777, Tehran, Iran

<sup>3</sup> CNRS UMR 6529, Observatoire de la Côte d'Azur, BP 4229, 06304 Nice Cedex 4, France

<sup>4</sup> Department of Physics, Iran University of Science and Technology, Narmak, Tehran 16844, Iran

<sup>5</sup> Institute for Advanced Studies in Basic Sciences, PO Box 45195-159, Zanjan, Iran

Received 26 July 2002, in final form 28 January 2003

Published 17 March 2003

Online at [stacks.iop.org/JPhysCM/15/1889](http://stacks.iop.org/JPhysCM/15/1889)

## Abstract

The spatial scaling law and intermittency of the  $V_2O_5$  surface roughness has been investigated by atomic force microscopy. The intermittency of the height fluctuations has been checked by two different methods, first, by measuring the scaling exponent of the  $q$ th moment of height-difference fluctuations i.e.  $C_q = \langle |h(x_1) - h(x_2)|^q \rangle$ , and second, by defining the generating function  $Z(q, N)$  and generalized multi-fractal dimension  $D_q$ . These methods predict that there is no intermittency in the height fluctuations. The observed roughness and dynamical exponents can be explained by numerical simulation on the basis of the forced Kuramoto–Sivashinsky equation.

(Some figures in this article are in colour only in the electronic version)

## 1. Introduction

Due to the technical importance and fundamental interest, a great deal of effort has been devoted to understanding the mechanism of thin-film growth and the kinetic roughening of growing surfaces in various growth techniques. Analytical and numerical treatments of simple growth models suggest, quite generally, that the height fluctuations have a self-similar character and their average correlations exhibit a dynamic scaling form [1–6].

Vanadium pentoxide,  $V_2O_5$ , has been the subject of intense work because of its diverse applications in catalytic oxidation reactions, cathodic electrodes in solid state micro-batteries, windows and electrochromic devices as well as gas sensors and its interest for transmittance modulation in smart windows with potential application in the architecture and automotive industries. Also  $V_2O_5$  is a low mobility semiconductor, having predominantly an n-type. Electrons are the charge carriers, and an increase in the carrier density is accompanied by reduction in oxygen concentration in the lattice [7–9].

This work aims to study the roughness and dynamical exponents ( $\chi$  and  $z$ ) and the intermittency of the  $V_2O_5$  films by atomic force microscopy. We measure the height-difference

moments  $C_q(l = |x_1 - x_2|) = \langle |h(x_1) - h(x_2)|^q \rangle$  and show that they behave as  $\sim |x_1 - x_2|^{\xi_q}$ . The obtained  $\xi_q$  is a linear function of  $q$ . We also introduce the generating function  $Z(q, N)$  and generalized multifractal dimension  $D_q$  and show that  $D_q$  also behaves as a linear function of  $q$ . These observations indicate that the height fluctuations are not intermittent. It is also argued that the measured roughness and dynamical exponents belong to the early-time scaling regime of the noisy Kuramoto–Sivashinsky (KS) equation.

## 2. Experiments

V<sub>2</sub>O<sub>5</sub> layers were grown on the polished Si(100) substrate by the resistive evaporation method in a high vacuum chamber. The pressure during evaporation was 10<sup>-5</sup> Torr. The thickness of the growing films was measured *in situ* by a quartz crystal thickness monitor. We performed all deposition at room temperature, with deposition rate about 10–15 nm min<sup>-1</sup>. However, during the film deposition the substrate temperature rose to  $T \sim 60^\circ\text{C}$ , due to the radiation effect of the alumina boat. The substrate temperature was determined using a chromel/alumel thermocouple mounted in close proximity to the samples. The surface composition of samples was measured by Auger electron spectroscopy (AES) using a 3 keV electron beam and a cylindrical mirror analyser (Varian model 981-2607). The surface topography of the films was investigated using a Park Scientific Instruments model Autoprobe CP. The images are collected in a constant force mode and digitized into 256 × 256 pixels with scanning frequency of 0.6 Hz. A cantilever of 0.05 N m<sup>-1</sup> spring constant with a commercial standard pyramidal Si<sub>3</sub>N<sub>4</sub> tip has been used. A variety of scans, each with size  $L$ , were recorded at random locations on the V<sub>2</sub>O<sub>5</sub> film surface. In order to determine the structure of the deposited V<sub>2</sub>O<sub>5</sub> films, we have performed XRD measurements of samples. The spectra for the as-deposited V<sub>2</sub>O<sub>5</sub> films grown showed that the V<sub>2</sub>O<sub>5</sub> thin films are amorphous. For thick films ( $d > 200$  nm) two very broad weak peaks were observed representing the growth of (001) and (002) peaks of the V<sub>2</sub>O<sub>5</sub> orthorhombic structure [7]. The yellow colour of deposited oxide films and their optical transmission spectra indicates the existence of V<sub>2</sub>O<sub>5</sub> structure rather than other vanadium oxide phases [8]. AES analysis of the V<sub>2</sub>O<sub>5</sub> samples showed V and O peaks at the surface of the deposited films. The stoichiometry of the vanadium oxide films was calculated from the ratio of O to V Auger peak heights by considering the elemental sensitivity factors. The O/V ratio was  $2.5 \pm 0.1$ , indicating the formation of stoichiometric vanadium pentoxide at the surface of the thin film (see figure 1). With these observations we conclude the film composition is nearly stoichiometric [9].

## 3. Results

Figure 2 shows the variation of the surface morphology for different growth times (or thicknesses) of processed samples by AFM. As deposition proceeds, the size of mountains and valleys grows until the system approaches a stationary state in which the thickness is about 150 nm.

The quantitative information of the surface morphology can be derived by considering a sample of size  $L$ , and defining the mean height of growing film  $\bar{h}$  and its roughness  $w$  through [10]

$$\bar{h}(L, t) = \frac{1}{L} \int_{-L/2}^{L/2} dx h(x, t) \quad (1)$$

and

$$w(L, t) = (\langle (h - \bar{h})^2 \rangle)^{1/2}. \quad (2)$$

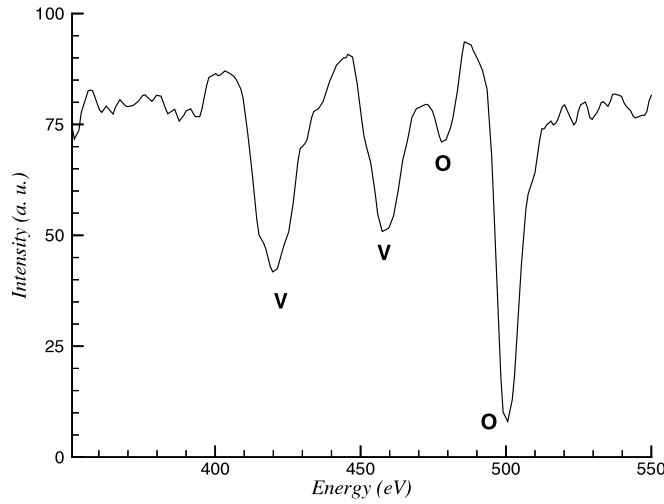


**Figure 1.** AES spectra from the V<sub>2</sub>O<sub>5</sub> surface. The O/V ratio is  $2.5 \pm 0.1$  (by considering the elemental sensitivity factors).

$\langle \dots \rangle$  denotes an averaging over different realizations (samples). Starting from a flat interface (one of the possible initial conditions), it was conjectured by Family and Vicsek [11] that a scaling of space by a factor  $b$  and of time by a factor  $b^z$  ( $z$  is the dynamical scaling exponent) re-scales the roughness  $w$  by a factor  $b^\chi$  as follows:  $w(bL, b^z t) = b^\chi w(L, t)$ , which implies that

$$w(L, t) = L^\chi f(t/L^z). \quad (3)$$

If for large  $t$  and fixed  $L$  ( $t/L^z \rightarrow \infty$ )  $w$  saturates, then  $f(x) \rightarrow \text{constant}$ , as  $x \rightarrow \infty$ . However, for a fixed large  $L$  and  $1 \ll t \ll L^z$ , one expects that correlations of the height fluctuations are set up only within a distance  $t^{1/z}$  and thus must be independent of  $L$ . This implies that for  $x \ll 1$ ,  $f(x) \sim x^\beta$  with  $\beta = \chi/z$ . Thus dynamic scaling postulates that  $w(L, t) \sim t^\beta$  for  $1 \ll t \ll L^z$  and  $\sim L^\chi$  for  $t \gg L^z$ . The roughness exponent  $\chi$  and the dynamic exponent  $z$  characterize the self-affine geometry of the surface and its dynamics, respectively. We measure the exponent  $\chi$  from the equal-time height–height correlation function defined as  $C_2(l = |x_1 - x_2|) = \langle |h(x_1) - h(x_2)|^2 \rangle$ . Here  $h(x)$  is the surface height at position  $x$  on the surface relative to the mean surface height.

In order to determine the roughness exponent  $\chi = \xi_2/2$ , we consider the roughness of the samples with thickness 20, 100 and 260 nm. Figure 3 shows that for the thicknesses 20 and 100 nm the scaling behaviour only exists for the scaling region  $\sim 4$ –20 nm, but for the stationary state sample,  $\langle h \rangle = 260$  nm, there is a cross over for the scaling exponent  $\chi = \xi_2/2$  in  $l = l_* \approx 22$  nm. The exponent is  $\xi_{21}$  for the length scales 4 nm to the scale  $l_*$ , and for the length scales  $25 \text{ nm} \leq l \leq 50 \text{ nm}$  the fluctuation is determined by another exponent  $\xi_{22}$ . The measured values for the exponents  $\xi_{21}$  and  $\xi_{22}$  are  $1.64 \pm 0.06$  ( $\chi_1 = 0.83 \pm 0.03$ ) and  $0.58 \pm 0.08$  ( $\chi_2 = 0.29 \pm 0.04$ ) respectively. The measured roughness exponents  $\chi$  of the 20, 100 and 150 nm samples are  $0.71 \pm 0.04$ ,  $0.77 \pm 0.03$  and  $0.82 \pm 0.03$ , respectively. As shown in figures 4 and 5, we note that the correlation length  $l_*$  is about 22 nm. Therefore, we are dealing with the statistical properties of the correlated scaling surfaces. As discussed in [22], such systems exhibit sampling-induced hidden cycles (log-periodic fluctuations [23]). Such oscillatory behaviour will diminish when the sampling size is sufficiently large. The oscillation amplitude approaches zero to within an order of  $\delta = \sqrt{l_* / ML}$ , where  $L$  and  $M$  are the

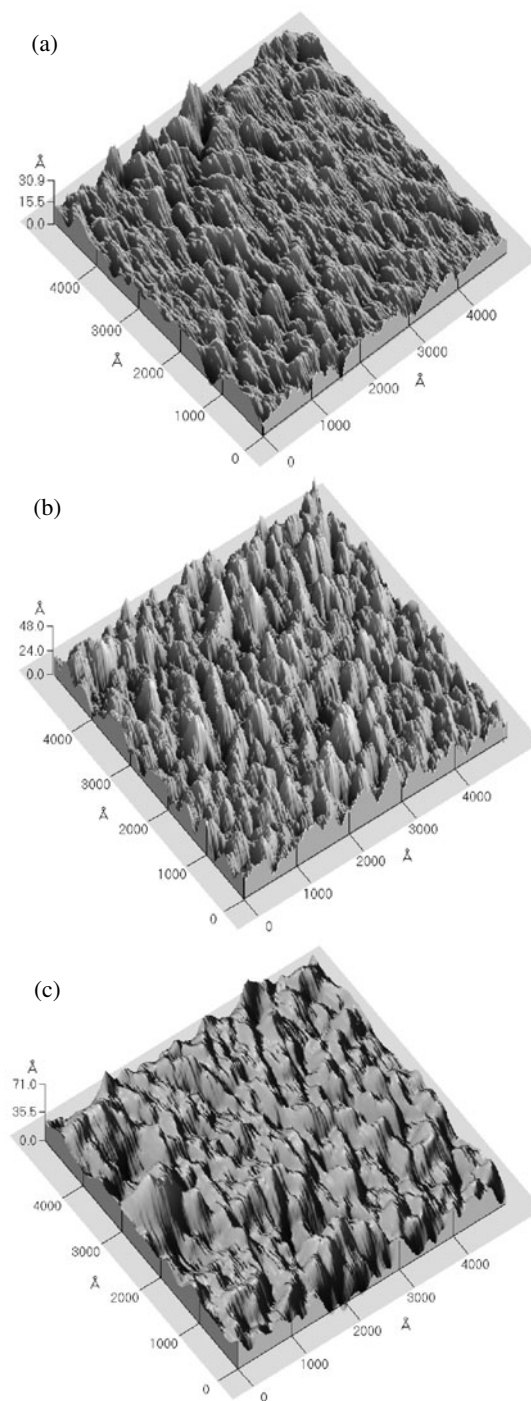


**Figure 2.** AFM surface images (all  $0.5 \times 0.5 \mu\text{m}^2$ ) of  $\text{V}_2\text{O}_5$  films with thicknesses of (a) 20 nm, (b) 100 nm and (c) 260 nm (from top to bottom).

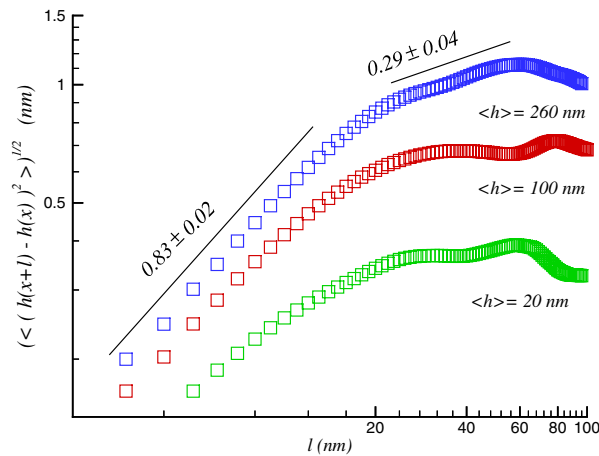


**Figure 3.** Log–log plot of the second moment of height difference versus  $l$ , which shows that for samples with thicknesses 20 and 100 nm the scaling region is  $4 \text{ nm} < l < 20 \text{ nm}$  and for the sample with thickness 260 nm there is a cross over scale  $l^* \approx 22 \text{ nm}$ . The upper and lower parts of height–height correlation function have the roughness exponent  $0.29 \pm 0.04$  and  $0.83 \pm 0.03$ , respectively.

sampling size and the number of independent curves which are averaged. We have determined each exponent by averaging over the eight AFM images. In our averaging it appears that there is no log-periodic property for the height–height correlation function. Therefore the surfaces of V<sub>2</sub>O<sub>5</sub> are self-affine.

The existence of the cross over scale  $l^*$  in the stationary state is not only observed in the second moment  $C_2$ . In figure 4 log–log plots of  $C_3$  versus  $l$  for the three samples are presented. It is evident that for the stationary state sample, the scaling exponent of the third moment  $C_3$  also has a cross over in  $l^*$ . The measurement shows that in the stationary state the exponents  $\xi_{3i}$  behave as  $\xi_{3i} = 3/2\xi_{2i}$  with  $i = 1, 2$ .

We also examine the scaling behaviour of the  $q$ th moment of the height difference  $C_q = \langle |h(x_1) - h(x_2)|^q \rangle$  and show that all of the moments at least up to  $q = 20$  behave as  $|x_1 - x_2|^{\xi_q}$ . Figure 5 shows  $\xi_q$  versus  $q$  for the 260 nm sample in the  $25 \text{ nm} \leq l \leq 50 \text{ nm}$  scaling region. The graph of  $\xi_q$  for the  $4 \text{ nm} \leq l \leq 20 \text{ nm}$  region is the same as figure 5 but with different slope. In the two scaling regions, the  $\xi_q$  have a linear dependence on  $q$ . This measurement indicates that the height fluctuations are not intermittent and all of the scaling exponents in the stationary state can be expressed by  $\xi_{2i}$ ,  $i = 1, 2$  only.

There is another method to check that the intermittency is absent in the height fluctuations of the V<sub>2</sub>O<sub>5</sub> surface [12, 13]. Let us introduce the generating function  $Z(q, N; l)$ . The generating function is defined through

$$Z(q, N; l) = \sum_{i=1}^N \mu_i^q, \quad (4)$$

where the normalized measure  $\mu_i \geq 0$  is

$$\mu_i = \frac{|h(x_i + l) - h(x_i)|}{\sum_{i=1}^N |h(x_i + l) - h(x_i)|}, \quad (5)$$

and  $N$  is the number of data  $|h(x_i + l) - h(x_i)|$ . For large  $N$ , the generating function  $Z$  scales as  $Z(q, N; l) \sim N^{-\tau(q)}$ . We measure the exponent  $\tau(q) = (q - 1)D_q$  in both scaling regions

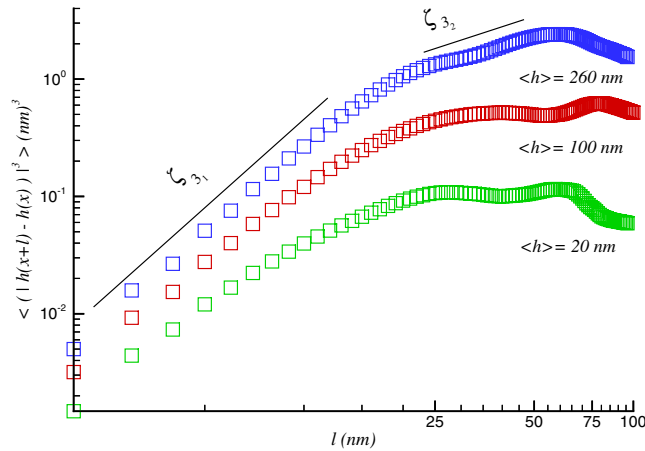


**Figure 4.** Log–log plot of the third moment of height difference versus  $l$ , which shows that in the length scale  $l^* \approx 22$  nm there is also a cross over for the scaling exponent  $\xi_3$  of the sample 260 nm.

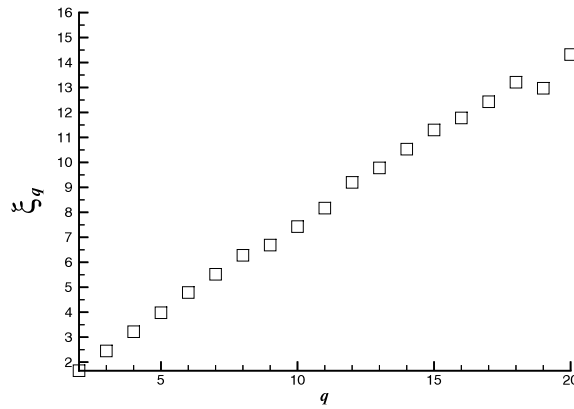


**Figure 5.** The plot of  $\xi_q$  versus  $q$ , which has a linear dependence on  $q$  and shows that the height-difference fluctuations are not intermittent.

(4–20 nm and 25–50 nm). The amplitude of  $Z$  depends only on  $l$  and  $q$ . In figure 6 we plot  $(1 - q)D_q$  versus  $q$  for small  $l$ . The figure shows that  $\tau(q)$  has a linear dependence on  $q$  and the generalized fractal dimension  $D_q$  is independent of  $q$ . Its value is  $D_q = D_0 = 7.34 \pm 0.02$ . Therefore, we conclude that the height fluctuation is not intermittent. It is necessary to note that the exponents  $\xi_q$  and  $D_q$  are not independent in the small region of  $l$ . Defining  $\xi_q = qH_q$ , it has been shown in [20] that  $H_q$  can be expressed in terms of  $D_q$  as

$$H_q = H_1 + \frac{(q - 1)(D_q - D_{eff})}{q}. \tag{6}$$

Our measurement for  $H_q$  shows that  $H_q$  is independent of  $q$  and this means that  $D_{eff} = D_q = D_0$ . Let us discuss the origin of  $D_{eff}$  in equation (6). To evaluate  $C_q$  we should calculate the summation  $\frac{1}{N} \sum_{i=1}^N |h(x_i) - h(x_i + l)|^q$ , where  $N$  is the number of points over which the average is taken. Normally small  $l$  is meant by  $l \sim 1/N$ . The authors of [20] assumed that, in evaluation of  $C_q$ ,  $l$  and  $N$  may be related in a way different from  $l \sim 1/N$ . That is,  $N \sim l^{-D_{eff}}$  ( $D_{eff}$  could be considered here as a fractal dimension of the effective support of the process).

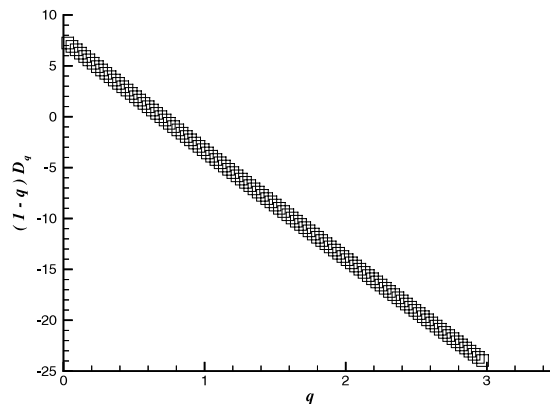


**Figure 6.** Plot of  $(1-q)D_q$  versus  $q$ , shows that the fluctuations are determined only by dimension  $D_0$  and the surface are not intermittent in the scaling region.

The choice of a particular partition has no effect on the  $H_q$  spectrum. However,  $D_{eff}$  enters the relation between  $H_q$  and generalized dimension  $D_q$  as expressed in equation (6).

#### 4. Discussion and growth model

In our experiments we obtain a region in which the growth exponents of V<sub>2</sub>O<sub>5</sub> are consistent with the early-scaling regime of the forced KS equation in 2 + 1 dimensions [19]. The forced KS has the following form [14–19]:

$$\frac{\partial h}{\partial t} = \nu \nabla^2 h - k \nabla^4 h + (\lambda/2)(\nabla h)^2 + \eta(x, t) \quad (7)$$

where  $\nu$ ,  $k$  and  $\lambda$  are the surface tension, surface diffusion and non-linear factor, respectively. The force  $\eta$  is a noise term reflecting spatial and temporal fluctuation in the incoming flux of material and has a Gaussian distribution and is uncorrelated in space and time. In the limit  $k = 0$  and for  $\nu > 0$  the forced KS equation reduces to the Kardar–Parisi–Zhang (KPZ) equation. The KS equation with  $\lambda = 0$  is a linear equation and can be exactly solved by the standard methods [19, 22]. For some Gaussian noise term, because of the linearity the probability distribution function (PDF) of  $h - \bar{h}$  is also Gaussian. It is discussed in [22] that for  $\lambda = 0$  and  $\nu/k < 0$  the KS equation generates a mound surface and for  $\nu/k > 0$  it gives a self-affine surface, with a roughness exponent  $\simeq 1$ . For  $\lambda \neq 0$  the nonlinear term breaks the symmetry under transformation  $h \rightarrow -h$ . Therefore the PDF of  $h - \bar{h}$  must be skewed. Our measured value for the PDF of  $h - \bar{h}$  shows that the PDF has positive skewness. We will report the skewness and kurtosis of the PDF of the V<sub>2</sub>O<sub>5</sub> films elsewhere [12].

Recent simulation of the KS equation reveals the presence of the early and long scaling regimes [19]. The initial-time values for the growth exponent  $\beta$  and the roughness exponent  $\chi$  are found to be 0.22–0.25 and 0.75–0.80 respectively. The long-time scaling regime is determined by the exponents  $\beta = 0.16$ –0.21 and  $\chi = 0.25$ –0.28. The scaling exponents are notably less than the exponents of KPZ equation [19]. The long-time behaviour of the KS-equation has an interesting feature. For long times the height–height correlation function exhibits a bifractal structure with two different roughness exponents (see figure 11 in [19]). For  $\lambda = 2.0$ ,  $\nu = -0.2$  and  $k = 2.0$ , the upper and lower parts of the height–height correlation function have the roughness exponents 0.27 and 0.71, respectively.



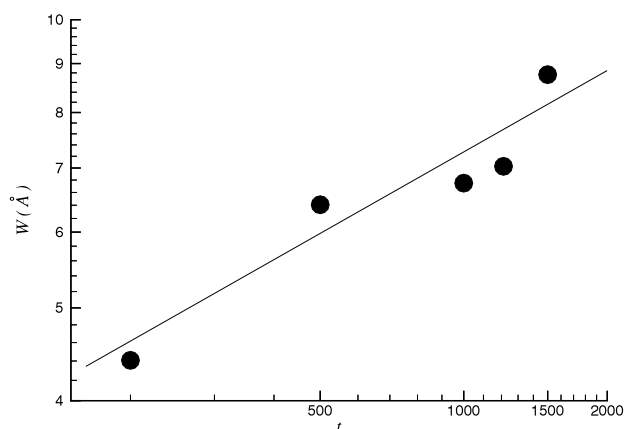


**Figure 7.** Log–log plot of the interface width  $w$  versus deposition time or thickness (in Å)  $t$  for the samples with thicknesses 20, 50, 100, 120 and 150 nm. The measured value for  $\beta$  is  $0.29 \pm 0.04$ .

Now let us compare our results with the numerical simulation of the KS equation. Using the numerical results of [19] in table 2, one can observe that for the early-scaling regime of the KS equation the exponents  $\chi$  and  $z$  satisfy the exponent-identity  $\chi + z \simeq 4$ . Using the time dependence of roughness of the samples with thicknesses 20, 50, 100, 120 and 150 nm we find that  $\beta = 0.29 \pm 0.04$  (see figure 7) and therefore  $\chi + z = 3.7 \pm 0.4$ , which satisfies the exponent-identity within the experimental errors. We also observe the similar bifractal structure of the height–height correlation function in our samples with thickness 260 nm (see figure 11 in [19]). To relate the cross over scale  $l^*$  to the surface morphology, we have measured the average distance of the nearest local maximum  $\bar{d}_{max}$ , and obtain that  $\bar{d}_{max}$  is of the same order of magnitude as  $l^*$ . This means that, in the stationary state, on average, if the distance between the points  $x_1$  and  $x_2$  lies between the two local maxima of  $h(x)$ , the dynamics is determined by the roughness exponent  $\chi_1$ . Also, for the points where the relative distance lies between the next neighbour maxima ( $\sim 20$ – $40$  nm), the dynamics is given by another exponent  $\chi_2$  which is less than the KPZ roughness exponent. Our measurements show that the roughness exponent  $\chi_2 = 0.29 \pm 0.04$  is less than the the KPZ roughness exponent in  $2 + 1$  dimensions i.e. 0.38.

In summary we have checked the intermittency of height fluctuation of  $V_2O_5$  via two different methods. These methods predict that the statistics of height fluctuations is not intermittent. We measure the scaling exponents of height-difference moments,  $C_q$  ( $l = |x_1 - x_2|$ ), and show that for small  $l$  they behave as  $\sim |x_1 - x_2|^{\xi_q}$ . The obtained  $\xi_q$  are linear functions of  $q$ . The observation can be explained with the recent numerical simulation on the basis of nonlinear KS equation. However, one should note that for very early stages, when the  $\nu$  term dominates the  $k$  term, instability arises in the  $x$  or  $y$  direction causing the ripple structure with corresponding wavevector in the  $x$  or  $y$  direction in the KS equation. When the ripple structure is formed, there exists slope asymmetry that activates the nonlinear effect. Therefore, in the early stage of the process, the ripple structure transforms to symmetric mounds. In our experiments we were not able to detect the ripple structure for the samples with  $\langle h \rangle \ll 20$  nm. This could mean that the polished Si(100) substrate may have an initial roughness which may destroy the ripple structure of the film for very early stages of the growth. We measure the roughness exponent of the silicon substrate and find that  $\chi_{Si} = 0.47 \pm 0.03$  (see figures 8 and 9).

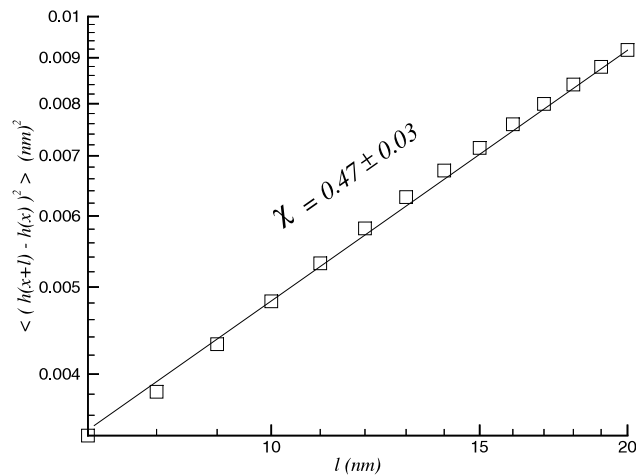


**Figure 8.** Log-log plot of the second moment of height difference versus  $l$ , for polished Si(100) substrate. The measured value for the roughness exponent is  $\chi_{Si} = 0.47 \pm 0.03$ .

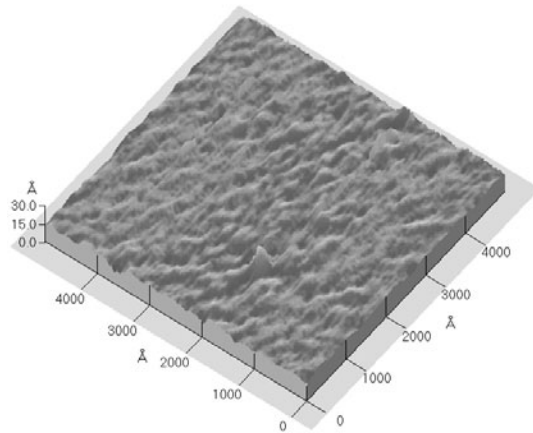


**Figure 9.** AFM image of polished Si(100) substrate.

Finally, we note that the measured roughness exponents  $\chi$  and  $\beta$  can be higher than the true values because of the tip effect [21]. Aue and De Hosson showed that the surface fractal dimension (fractal dimension  $d_f$  for a  $2 + 1$  interface is related to  $\chi$  by  $d_f = 3 - \chi$ ) determined with a scanning probe technique will always lead to an underestimate of the actual fractal dimension, due to the convolutions of tip and surface. Their analysis included tips with different shapes and aspect ratios. For a tip similar to what we have used, it is suggested that our true  $\chi_1$  and  $\chi_2$  should be around  $\sim 0.75$  and  $\sim 0.25$ , respectively. We note that the corrected exponents also satisfy the exponent identity.

### Acknowledgments

We thank A Aghamohammadi, F Azami, M M Ahadian, J Davoudi, A Farahzadi, G Ketabi and Z Vashaei for useful discussions.

## References

- [1] Barabasi A-L and Stanley H E 1995 *Fractal Concepts in Surface Growth* (New York: Cambridge University Press)
- [2] Halpin-Healy T and Zhang Y C 1995 *Phys. Rep.* **245** 218
- [3] Krug J 1997 *Adv. Phys.* **46** 139
- [4] Krug J and Spohn H 1990 *Solids Far from Equilibrium Growth, Morphology and Defects* ed C Godreche (New York: Cambridge University Press)
- [5] Meakin P 1998 *Fractal, Scaling and Growth Far from Equilibrium* (Cambridge: Cambridge University Press)
- [6] Kardar M 2000 *Physica A* **281** 295
- [7] Masoudi A A, Shahbazi F, Davoudi J and Reza Rahimi Tabar M 2002 *Phys. Rev. E* **65** 026132
- [8] Benmoussa M, Ibnouelghazi E, Bennouna A and Ameziane E L 1995 *Thin Solid Films* **265** 22
- [9] Aly S A, Mahmoud S A, El-Sayed N Z and Kaid M A 1999 *Vacuum* **55** 159
- [10] Svitashva S N and Kruchinin V N 1998 *Thin Solid Films* **313/314** 319
- [11] Marsilli M, Maritan A, Toigoend F and Banavar J R 1996 *Rev. Mod. Phys.* **68** 963
- [12] Family F and Vicsek T 1985 *J. Phys. A: Math. Gen.* **18** L75
- [13] Irajizad A, Kavei G, Reza Rahimi Tabar M and Vaez Allaei S M 2003 in preparation
- [14] Lee J and Stanley H E 1988 *Phys. Rev. Lett.* **61** 2945
- See also
- [15] Bunde A and Havlin S (ed) 1991 *Fractal and Disordered Systems* (Berlin: Springer) p 15
- [16] Bradley R M and Harper J M E 1994 *J. Vac. Sci. Technol. A* **6** 2390
- [17] Cuerno R and Barabasi A-L 1995 *Phys. Rev. Lett.* **74** 4746
- [18] Cuerno R, Makse H A, Tommasone S, Harrington S T and Stanley H E 1995 *Phys. Rev. Lett.* **75** 4464
- [19] Lauritsen K B, Cuerno R and Makse H A 1996 *Phys. Rev. E* **54** 3577
- [20] Anthony C-T, Chan A and Wang G-C 1998 *Surf. Sci.* **414** 17–25
- [21] Drotar J T, Zhao Y-P, Lu T-M and Wang G-C 1999 *Phys. Rev. E* **59** 177
- [22] Barabasi A-L, Szeffalussy P and Vicsed T 1991 *Physica A* **178** 17
- [23] Bershadskii A 1998 *Phys. Rev. E* **58** 2660
- [24] Aue J and De Hosson J Th M 1997 *Appl. Phys. Lett.* **71** 1347
- [25] Yang H-N, Zhao Y-P, Chan A, Lu T-M and Wang G-C 1997 *Phys. Rev. E* **56** 4224
- [26] Abed-pour N, Aghamohammadi A, Khorrani M and Reza Rahimi Tabar M 2003 *Nucl. Phys. B* **653** 342